The Cryosphere Discuss., 9, 45–75, 2015
www.the-cryosphere-discuss.net/9/45/2015/
doi:10.5194/tcd-9-45-2015

The Cryosphere Discussions
Open Access

Winter observations of CO_2 exchange between sea-ice and the atmosphere in a coastal fjord environment

J. Sievers[1,3], L. L. Sørensen[1,3], T. Papakyriakou[5], M. K. Sejr[2,3], D. H. Søgaard[4,7], D. Barber[5], and S. Rysgaard[3,4,5,6]

[1]Department of Environmental Science, Aarhus University, 4000 Roskilde, Denmark
[2]Department of Bioscience, Aarhus University, 8600 Silkeborg, Denmark
[3]Arctic Research Centre, Aarhus University, 8000 Aarhus, Denmark
[4]Greenland Climate Research Centre, c/o Greenland Institute of Natural Resources box 570, Nuuk, Greenland
[5]Centre for Earth Observation Science, CHR Faculty of Environment Earth and Resources, University of Manitoba, 499 Wallace Building Winnipeg, MB R3T 2N2, Canada
[6]Department of Geological Sciences, University of Manitoba, Winnipeg, Winnipeg, MB R3T 2N2, Canada
[7]Department of Biology, University of Southern Denmark, Campusvej 55, 5230 Odense M, Denmark

Received: 26 November 2014 – Accepted: 9 December 2014 – Published: 6 January 2015

Correspondence to: J. Sievers (jasi@dmu.dk)

Published by Copernicus Publications on behalf of the European Geosciences Union.

Abstract

Eddy covariance observations of CO_2-fluxes were conducted during March–April 2012 in a temporally sequential order at three locations on fast sea-ice and on newly formed polynya ice in a coastal fjord environment in North East Greenland. CO_2 fluxes at the three sites, ICEI, POLYI and DNB, were found to increase over time in accordance with the progression of springtime warming: $F_{CO_2}^{ICE1} = 1.4 \pm 4.9\,mmol\,m^{-2}\,d^{-1}$, $F_{CO_2}^{POLY1} = -3.4 \pm 31.4\,mmol\,m^{-2}\,d^{-1}$ and $F_{CO_2}^{DNB} = 36.7 \pm 72.8\,mmol\,m^{-2}\,d^{-1}$, where values given are the mean and SD, and negative/positive values indicate uptake/outgassing respectively. Observations were carried out at the three sites for 8, 4 and 30 days respectively. A correlation analysis indicates a strong connection between net radiative forcing, wind-speed and CO_2-fluxes. Correlations between latent heat fluxes and CO_2-fluxes were found for the first time and support the presence of adsorption/desorption processes of CO_2 in moist snow.

1 Introduction

Sea-ice has long been considered a passive participant in the high latitude carbon cycle, preventing CO_2 exchange between the ocean and atmosphere. Consequently, most carbon-cycle research has treated ice-cover as areas of zero (or very low) exchange (Tison et al., 2002). This view has been challenged by reports of significant fluxes of CO_2 over first and multiyear sea-ice during both spring/summer (Delille et al., 2007; Geilfus et al., 2012; Papakyriakou and Miller, 2011; Semiletov et al., 2004, 2007; Zemmelink et al., 2006) and autumn/winter (Else et al., 2011; Geilfus et al., 2013; Miller et al., 2011a, b) and suggestions of a coupling between the carbonate system in sea ice, the underlying sea water and the atmosphere (Anderson et al., 2004; Nomura et al., 2006; Papadimitriou et al., 2004; Rysgaard et al., 2011, 2012, 2007, 2013).

The coupling of the air–ice–ocean carbonate system has been suggested to drive a significant annual net uptake of CO_2, through convective sequestration of CO_2 to

TCD
9, 45–75, 2015

intermediate and deeper ocean layers during wintertime sea ice formation and subsequent CO_2 uptake from the atmosphere during springtime sea-ice melt (Rysgaard et al., 2009, 2007). Together with seasonal biological carbon uptake within the ice (Thomas and Dieckmann, 2010; Lizotte, 2001), this outlines the basis for a seasonal carbon imbalance, which may drive CO_2 uptake from the atmosphere during springtime melting of sea-ice, and mineral dissolution of trapped calcium carbonate ($CaCO_3$) within the brine channels. The net uptake associated with this sea ice-driven carbon pump has been estimated to be 50 MT C yr^{-1} in the Arctic alone (Rysgaard et al., 2007) and constitutes an important fraction of the total CO_2 uptake of the Arctic Ocean (66–199 MT C yr^{-1}) (Parmentier et al., 2013). This highlights the importance of the annual sea ice cycle on the global carbon cycle, particularly since the sea ice cover is becoming more ephemeral over a range of space and time scales (Barber et al., 2014).

Accurate assessment of the impact of air–ice–ocean CO_2 exchanges on the global carbon budget in a future climate requires the continued advancement of exchange parameterizations and up-scaling techniques that describe exchange dynamics within all sea-ice conditions as well as particularly dynamic areas such as polynyas, leads, cracks and thaw-holes. To our knowledge only one attempt has been made at developing a parameterization for air–sea ice CO_2 exchanges (Sørensen et al., 2014). This study emphasizes the importance of, and difficulties in, estimating the surface pCO_2 concentration in sea ice in order to make a proper parameterization. In general there is a need for further investigations into the interplay between biogeochemical and physical processes in facilitating and mediating observed air–sea ice CO_2 exchanges. Such efforts are, however, complicated by the logistical limitations associated with conducting large-scale observations in the Arctic, and the prerequisite requirement of providing trustworthy data from an inhospitable and instrument-challenging environment. From a surface-flux perspective, recent studies have suggested that some open path infrared gas analyzers, commonly used to conduct eddy covariance observations (e.g. Baldocchi, 2008) of CO_2 fluxes, may be subject to sensor bias during cold weather application (Papakyriakou and Miller, 2011, and references herein). A recent study fur-

TCD
9, 45–75, 2015

thermore found that eddy covariance flux estimates in environments characterized by very small scalar fluxes, such as sea ice, are likely to be influenced by larger scale motions, making it difficult to accurately resolve vertical turbulent fluxes under these conditions (Sievers et al., 2014).

Here we present an investigation into connections between site surface energetics, wind speed and CO_2 fluxes over snow covered sea ice during a 6 week field experiment in late winter (March–April) of 2012 in the fast sea ice and polynya environment of Young Sound, NE Greenland. Measurements were conducted with gas analyzers believed to be less sensitive to temperature biases relative to previous reported studies and eddy covariance flux estimates were derived using the Ogive optimization method (Sievers et al., 2014) which accounts for the problem of influence from large scale motions in low-flux environments.

2 Theory and method

2.1 Study location and instrumentation

Observations of CO_2-exchanges were carried out from early March to late April of 2012 in the vicinity of the Daneborg base in Young Sound, NE Greenland (Fig. 1). During the campaign two separate flux towers, one stationary and one mobile, were used at three different locations (ICEI, POLYI and DNB). ICEI and POLYI were represented in a recent study concerning the distribution of ikaite crystals ($CaCO_3 \cdot H_2O$) in sea ice (Rysgaard et al., 2013). Data were collected at ICEI (74°18.576′ N, 20°18.275′ W) and DNB (74°18.566′ N, 20°13.998′ W) from the 20–27 March and the 29 March to the 27 April respectively. Both were located inside Young Sound in conditions of 110–115 cm thick sea ice and 67–88 cm snow cover thickness. Data were collected at POLYI (74°13.883′ N, 20°07.758′ W) from the 24–27 March at the mouth of the sound in an active polynya area. Conditions at the site were distinctly different from those of ICEI

TCD
9, 45–75, 2015

and DNB, with 15–30 cm ice thickness and 15–20 cm snow cover thickness (Barber et al., 2014).

Observations of the three wind components and CO_2 at the static site (ICEI) were performed with a Gill Windmaster sonic (Gill Instruments®, Lymington UK) and an LI-7200 closed path gas analyzer (LI-COR®, Licoln, NE, USA), placed 3.8 and 3.5 m above the snow surface respectively, with a horizontal separation of 0.42 m. Observation frequency was 10 Hz. A number of datasets were discarded due to frosting on the sensors and unfavorable wind directions for which the flow was potentially disturbed by the tower itself. Net radiation was recorded with a Kipp & Zonen CNR1 net radiometer (Kipp & Zonen®, Delft, the Netherlands) placed 1.00 m above the undisturbed snow surface. Observations of the wind components and CO_2 at the mobile site (POLYI and DNB) were performed with a METEK USA-1 sonic anemometer (METEK®, Elmshorn, Germany) and a LI-7500A (LI-COR®, Licoln, NE, USA) gas analyzer, placed 3.1 and 2.7 m above the snow-surface, with a horizontal separation of 0.44 m. Observation frequency was 20 Hz. As at ICEI, a number of datasets were discarded because of frosting on the sensors and unfavorable wind direction. In addition to filtering for tower based flow distortion, observations from the shore-adjacent DNB site, reflecting wind-directions associated with the shoreline, were likewise filtered out due to anthropogenic interference. At the POLYI site net radiation was recorded with a Kipp & Zonen CNR1 net radiometer (Kipp & Zonen®, Delft, the Netherlands). At the DNB site no on-site net radiometer data were available. Over this period we make use of radiation measurements made with a Kipp & Zonen CMA6 and a Kipp & Zonen NR lite net radiometer (Kipp & Zonen®, Delft, the Netherlands) located in Zackenberg research station (74°28.315′ N, 20°33.125′ W), approximately 20 km further in-sound relative to the Daneborg base (Fig. 1). Air temperature was observed at ICEI and POLYI using Campbell Scientific HMP45C212 sensors (Campbell Scientific®, UT, USA). Chamber observations of CO_2 flux were carried out at sites ICEI and POLYI using an LI-8100A (LI-COR®, Licoln, NE, USA) automated soil CO_2-flux chamber system. Sea ice cores

TCD
9, 45–75, 2015

were extracted at all sites using a MARK II coring system (Kovacs Enterprises). Temperature readings were performed on all cores, while the sea ice cores from ICEI and POLYI were subjected to additional brine volume calculation as described in (Rysgaard et al., 2013).

2.2 Flux measurements and analysis

The surface flux estimates of CO_2, sensible and latent heat were derived using Ogive optimization (Sievers et al., 2014). The approach allows for separation of vertical turbulent flux and contributions from larger scale motions by optimization of a model Ogive spectral distribution (Desjardins et al., 1989; Foken et al., 2006) to a density distribution of a large number of Ogive spectral distributions (here 10 000), for which dataset length and de-trending by running mean are varied simultaneously. Flux estimates are discarded only if an excessive number of gaps are present in the raw dataset or if no theoretical model Ogive distribution can be optimized sufficiently. Here we adopt the standard convention that all turbulent fluxes are negative towards the surface and positive away from the surface.

2.3 The surface energy balance

Following e.g. (Else et al., 2014; Persson, 2012) the surface energy balance of snow overlaying sea-ice may be written as:

$$\Delta Q = -R_{\text{net}} - Q_{\text{SENS}} - Q_{\text{LAT}} - G \quad (1)$$

Where ΔQ is the net energy flux at the surface, $R_{\text{net}} = R_{\text{n}}^{\text{SW}} + R_{\text{n}}^{\text{LW}} - R^{\text{T}}$ is the net radiative flux, R_{n}^{SW} and R_{n}^{LW} are the net shortwave (0.3–5 µm) and longwave (5–40 µm) radiative fluxes respectively, R^{T} is the net radiative energy transmitted into the snow cover, Q_{SENS} is the turbulent sensible heat flux, Q_{LAT} is the turbulent latent heat flux and G is the upward conductive heat through the snow and ice. We deviate from Persson (2012) by treating all terms as positive if energy is transported away from the sur-

TCD
9, 45–75, 2015

face and negative otherwise, thus conforming to the conventions of turbulent fluxes, to simplify interpretation of a correlation analysis, which follows in a subsequent section. Using this notation, ΔQ, will be positive when net energy is received by the snow/ice volume, and negative when net energy is lost. While R_n^{LW}, Q_{SENS} and Q_{LAT} are exchanged virtually at the snow surface, R_n^{SW} penetrates into the snow/ice cover where it is strongly attenuated with depth. Following (Persson, 2012, Eq. 10) we can derive a 1 % transmission rate at 0.46 m depth into snow, suggesting that for very thick snow covers, energy transport to the snow/ice interface relies on other mechanisms. Energy transport within a snow cover occurs mainly as conduction between snow-grains and as vapour transport (Sturm et al., 2002). Upward vapour transport by thermal convection has been shown to occur in terrestrial snow covers (Powers et al., 1985; Sturm, 1991) and to depend on medium porosity and the strength of the temperature gradient within the medium (Ganot et al., 2014).

3 Observations

3.1 ICEI

Freeboard, which is the height of the ice above the water surface, was found at ICEI to be negative and a thin slush layer was observed at the snow/ice interface. Observed CO_2 fluxes, energy fluxes, and meteorological parameters from the site are shown in Fig. 2. The site experienced a number of power outages, primarily during night and in the morning, as indicated by instrument status bars (Fig. 2a). The prevailing wind direction (Fig. 2a) during the ICEI experiment was from the ice covered inner fjord (North). The period was dominated by low wind speeds on the order of 1–2 m s^{-1} with three events of relatively strong wind-speed U = 6–8 m s^{-1} recorded on the evening of the 20 March, past midday on the 25 March and during night on the 26 March respectively (Fig. 2a). Air temperature was recorded within the range $T_{air} = -25 \pm 10$°C and followed a diurnal pattern with daily temperature changes on the order of 10–

TCD
9, 45–75, 2015

15°C (Fig. 2a). The range of CO_2 fluxes observed at ICEI (Fig. 2a) was modest and characterized by limited variation; $F_{CO_2} = 1.4 \pm 4.9\,\mathrm{mmol\,m^{-2}\,d^{-1}}$, where values given are the mean and SD. Two chamber observations were conducted just before midday on the 25 March (Fig. 2a, magenta diamonds), both showing flux estimates similar to eddy covariance derived flux estimates at the same time during both the preceding and the following day ($F_{CO_2} = 0.86\,\mathrm{mmol\,m^{-2}\,d^{-1}}$ and $F_{CO_2} = 2.16\,\mathrm{mmol\,m^{-2}\,d^{-1}}$). No concurrent eddy covariance observations were available. Average net solar radiation during the experiment was low $\overline{R}_n^{SW} = -27\,\mathrm{W\,m^{-2}}$ (Fig. 2b). Sensible heat fluxes were predominantly within the range $Q_{SENS} = \pm 5\,\mathrm{W\,m^{-2}}$ with three events of strong warming and cooling $Q_{SENS} = \pm 25\,\mathrm{W\,m^{-2}}$ recorded on the evening of the 20 March, the evening and night of the 25–26 March and the night of the 26–27 March, respectively (Fig. 2c). The only non-negligible latent heat fluxes were recorded on the night of the 26–27 March within the range $Q_{LAT} = 2 \pm 2\,\mathrm{W\,m^{-2}}$ (Fig. 2c). Ice-temperatures taken from an extracted ice-core on the 17 March, three days before the initiation of the experiment, indicated a snow/ice interface temperature at −10°C and calculated brine volume at around $V_B = 5.1\,\%$ (Rysgaard et al., 2013).

3.2 Observations at POLYI

Freeboard at POLYI was found to be negative and a slush layer was observed at the snow/ice interface. The snow base was generally characterized by a higher level of moisture relative to the ICEI and DNB sites. Observed CO_2 fluxes, meteorological parameters and components of the energy balance from the site are shown in Fig. 3. The prevailing wind direction (Fig. 3a) during the entire experiment was from the ice covered inner fjord (West) and the period was dominated by low to moderate wind speeds within the range $U = 1$–$6\,\mathrm{m\,s^{-1}}$. Air temperature was recorded within the range $T_{air} = -17 \pm 8$°C and followed a diurnal pattern with daily temperature changes on the order of 10°C as well as a general incline of 5°C during the experiment (Fig. 3a). We note that due to the relatively thin snow cover and cold atmosphere, the ice at this site

TCD
9, 45–75, 2015

was actively growing, as opposed to the thicker inner-fjord sites ICEI and DNB. CO_2 fluxes observed at POLYI (Fig. 3a) were both larger and more variable relative to observations at ICEI; $F_{CO_2} = -3.4 \pm 31.4\,\mathrm{mmol\,m^{-2}\,d^{-1}}$, where values given are the mean and SD. Two chamber observations (Fig. 3a, magenta diamonds), performed on the ice and in the snow on the 25 March (Fig. 3a), both showed significantly smaller flux estimates (order of $|F_{CO_2}| \leq -3.5\,\mathrm{mmol\,m^{-2}\,d^{-1}}$) relative to concurrent eddy covariance derived fluxes. Average net solar radiation during the experiment was slightly stronger than at ICEI; $\overline{R}_n^{SW} = -40\,\mathrm{W\,m^{-2}}$ (Fig. 3b). Sensible heat fluxes were observed within the range $Q_{SENS} = \pm 25\,\mathrm{W\,m^{-2}}$ with three events of strong heating and cooling recorded on the evening/night of the 24 March, the midday/evening on the 25 March and the early morning on the 27 March (Fig. 3c). The only non-negligible latent heat fluxes were recorded on the morning of the 27 March within the range $Q_{LAT} = 2 \pm 2\,\mathrm{W\,m^{-2}}$ (Fig. 3c). An ice-core observation on the 20 March, five days before the initiation of eddy covariance measurements at POLYI, indicated a snow/ice interface temperature around −5 °C and calculated brine volume at around 12 % (Rysgaard et al., 2013).

3.3 Observations at DNB

Freeboard at DNB was found to be negative and a thin slush layer was observed at the snow/ice interface in the beginning of the measurement period. Observed CO_2 fluxes, meteorological parameters and components of the energy balance from the site are shown in Fig. 4. The prevailing wind direction (Fig. 4a) during the entire experiment was from the ice-covered inner fjord (North-West) and the period was dominated by low wind speeds of 1–4 $\mathrm{m\,s^{-1}}$ with three events of very strong wind-speed of 6–10 $\mathrm{m\,s^{-1}}$ recorded on the 29 March, the 9–10 April and on the 25–26 April respectively (Fig. 4a). Air temperature was recorded within the range of -19 ± 6 (Fig. 4a). The range of CO_2 fluxes observed at DNB (Fig. 4a) was the largest during the entire field-campaign; $F_{CO_2} = 36.7 \pm 72.8\,\mathrm{mmol\,m^{-2}\,d^{-1}}$, where values given are the mean and SD. Average net solar radiation during the experiment was significantly higher than for both

TCD
9, 45–75, 2015

ICEI and POLYI; $\overline{R}_{n}^{SW} = -75\,W\,m^{-2}$ (Fig. 4b). Sensible heat fluxes were predominantly within the range $Q_{SENS} = \pm 20\,W\,m^{-2}$ with two events of strong heating and cooling $Q_{SENS} = \pm 60\,W\,m^{-2}$ recorded between the 9–10 April and the 25–26 April (Fig. 4c). Latent heat fluxes were recorded within the range $Q_{LAT} = 3 \pm 3\,W\,m^{-2}$ (Fig. 4c). Temperature readings of ice-cores (K. Attard, unpublished) taken a couple of days before the initiation of observations at the DNB site on the 26 and 28 March respectively, indicated an increase in temperature from −4.7 to −4.0°C at the snow/ice interface.

4 Data analysis and discussion

4.1 On the size of the CO_2-fluxes

The CO_2-fluxes observed during this experiment, particularly at POLYI and DNB, are comparable to the larger flux-rates reported in past studies over sea ice; $F_{CO_2}^{ICE1} = 1.4 \pm 4.9\,mmol\,m^{-2}\,d^{-1}$, $F_{CO_2}^{POLY1} = -3.4 \pm 31.4\,mmol\,m^{-2}\,d^{-1}$ and $F_{CO_2}^{DNB} = 36.7 \pm 72.8\,mmol\,m^{-2}\,d^{-1}$. Using eddy covariance instrumentation, CO_2-fluxes within the range $\pm 60\,mmol\,m^{-2}\,d^{-1}$ have been measured over fast sea-ice near barrow, Alaska in June 2002 (Semiletov et al., 2004). CO_2-fluxes within the range $-11 \pm 18\,mmol\,m^{-2}\,d^{-1}$ have been observed in summer sea-ice from the western Weddell Sea, Antarctica (Zemmelink et al., 2006). CO_2-fluxes within the range $0.3 \pm 1.5\,mmol\,m^{-2}\,d^{-1}$ were observed from a drifting ice-station in the Laptev sea during September 2007 (Semiletov et al., 2007). Average CO_2-fluxes of $19.9\,mmol\,m^{-2}\,d^{-1}$ and $32 \pm 5.2\,mmol\,m^{-2}\,d^{-1}$ were observed on newly forming fast ice (30–40 cm thick) and on older fast ice respectively, in the Canadian arctic during November 2007 through January 2008 (Else et al., 2011). The authors also report strong uptake in areas of unconsolidated ice, open water and active leads. Daily average CO_2-fluxes within the range $7 \pm 67\,mmol\,m^{-2}\,d^{-1}$ were reported on growing fast ice (0.8–1.7 m thickness) in the Canadian arctic during January through June 2004 (Miller et al., 2011b). CO_2-fluxes within the range

TCD
9, 45–75, 2015

$-78 \pm 180\,\mathrm{mmol\,m^{-2}\,d^{-1}}$ were reported on first-year ice in the Canadian arctic during May through June 2002 (Papakyriakou and Miller, 2011). Using chamber instrumentation, CO_2-fluxes within the range $1.5 \pm 1.5\,\mathrm{mmol\,m^{-2}\,d^{-1}}$ were observed at ice-stations of various characteristics in the Canadian arctic during April through June 2008 (Geilfus et al., 2012). The disparity in strength and direction of observed CO_2-fluxes at sites of different characteristics and at different time of year confirm that sea-ice is a very dynamic system and that further studies are necessary to understand the full potential of sea-ice in offsetting both regional- and global-scale carbon cycles. It is also possible that some of the fluxes derived using eddy covariance in the studies cited above contained a heating bias (cf. Papakyriakou and Miller, 2011).

4.2 Processes controlling the CO_2 fluxes

4.2.1 Site energy fluxes

In order to investigate the association of the surface energy balance with CO_2 exchanges, we performed a correlation analysis (Fig. 5). For ICEI (Fig. 5a–e) all correlations are seen to be very small and no clear pattern between any of the energy balance components and CO_2-fluxes is evident. For POLYI (Fig. 5f–j), some clear patterns and convincing correlations are found. Most notably a strong negative correlation between CO_2-fluxes and the sensible heat-flux ($R^2 = 0.89$, $p < 0.05$) (Fig. 5f). A similar association was noted over Antarctic sea ice by (Zemmelink et al., 2006). A strong positive correlation between CO_2-fluxes and net radiative forcing ($R^2 = 0.73$, $p < 0.05$) was also observed. Specifically, surface net radiative cooling and downward sensible heat flux coincides with outgassing of CO_2, while surface net radiative warming and upward sensible heat flux coincides with uptake of CO_2. Moreover, there appears to be a strong correlation between latent heat fluxes and CO_2-fluxes at POLYI (Fig. 5g). If we disregard the cluster of apparent outliers, which stem from a lone case of non-negligible latent heat fluxes observed alongside negligible CO_2-fluxes in the morning of the 27 March (Fig. 3), the correlation becomes $R^2 = 0.72$, $p < 0.05$. At DNB

TCD
9, 45–75, 2015

(Fig. 5k–o) an almost perfect negative correlation between CO_2-flux and sensible heat flux ($R^2 = 0.94$, $p < 0.05$) (Fig. 5k) is observed. Also evident in the analysis is a strong positive correlation between CO_2-flux and net radiative forcing ($R^2 = 0.40$, $p < 0.05$) (Fig. 5o).

Brine volume decreases with decreasing sea-ice temperature. This can lead to significant changes in the mineral-liquid thermodynamic equilibrium of the brine and to thermally sequential mineral precipitation (Marion, 2001), most notably of calcium carbonate in the form of the metastable mineral *ikaite* ($CaCO_3 \cdot 6H_2O$) at temperatures below −2.2°C:

$$Ca^{2+} + 2HCO_3^- \leftrightarrow CaCO_3 + H_2O + CO_{2(aq)} \quad \text{(R1)}$$

The formation of $CaCO_3$ and $CO_{2(aq)}$ and the decreasing CO_2 solubility of the increasingly saline brine (Tison et al., 2002), drives the brine to higher CO_2 partial pressure (pCO_2) (Geilfus et al., 2012). Hence, the temperature sensitivity of carbon speciation in sea ice brines supports the premise that thermochemical processes within brine exposed to the atmosphere facilitates an air–ice pCO_2 gradient, thereby linking CO_2 exchange to site energetics via brine carbon chemistry (Loose et al., 2011). In theory, sea ice is permeable to vertical brine transport when brine proportion by volume in sea ice is in excess of ∼ 5 % (Golden et al., 1998). The brine–atmosphere interface may be positioned at the sea ice surface or at distance up into the snow pack as would be the case for brine-wetted snow. Snow over sea ice may contain appreciable quantities of salt, drawn up from the ice surface in the form of concentrated brine (Barber et al., 1995a, b; Crocker, 1984; Perovich and Richtermenge, 1994). A list of processes possibly affecting pCO_2 at the brine–atmosphere interface include; (1) given sufficiently permeable sea-ice (Golden et al., 1998; Loose et al., 2011a, b) brine concentration/dilution, alters the pCO_2 gradient across the sea-ice surface and thus the potential for CO_2 exchanges (Geilfus et al., 2012; Killawee et al., 1998; Tison et al., 2002; Nomura et al., 2006; Papadimitriou et al., 2004). (2) Formation/dissolution of calcium carbonate ($CaCO_3 \cdot 6H_2O$) within brine (Dieckmann et al., 2008; Fischer et al.,

TCD
9, 45–75, 2015

2013; Marion, 2001; Papadimitriou et al., 2004; Rysgaard et al., 2013) leads to an increase/decrease in brine pCO_2 thus changing the potential for CO_2 exchanges at the ice surface (Geilfus et al., 2012; Miller et al., 2011b; Papakyriakou and Miller, 2011; Sogaard et al., 2013). (3) $CaCO_3 \cdot 6H_2O$ has been observed in brine-soaked snow at the snow/ice interface (Fischer et al., 2013; Geilfus et al., 2013; Nomura et al., 2013). This suggests that formation/dissolution of $CaCO_3 \cdot 6H_2O$ in snow may be able to contribute to observed CO_2 exchange, particularly during conditions conducive to upward transport of brine to the snow base from the sea ice (e.g. large snow/ice interface brine volume and negative freeboard).

The fact that CO_2-fluxes at ICEI (Fig. 5a–e) were very close to zero may be because (1) calculated brine volume (Rysgaard et al., 2013) was just at the critical threshold for gas-permeability $V_B = 5.1\,\%$ (Golden et al., 1998; Loose et al., 2011a, b), raising the possibility that brine transport was inhibited within the ice during that part of the experiment, and (2) the thick overlying snow cover prevented the free exchange of CO_2 in absence of wind-induced ventilation. We discuss the latter issue below. On the other hand, the stronger fluxes observed at POLYI may be attributed to brine transport in response to the much larger calculated brine volumes $V_B = 12\,\%$. Vertical brine transport and possible mixing with under-ice sea ice water (Zhou et al., 2013; Vancoppenolle et al., 2010) provides a mechanism for the brine wetting of the snow/ice interface and possibly of the snow-base. In this situation brine is close to the snow/atmosphere interface, not only allowing for an enhanced CO_2 exchange with the atmosphere, but also subject to more pronounced temperature shifts in response to the 24 h cycle of the diurnal energy budget at the site. As mentioned, changes in brine solubility of CO_2 and the dissolution/precipitation of $CaCO_3 \cdot 6H_2O$ associated with changing temperature provides for a dynamic air–ice pCO_2 gradient.

Brine salinity and density increases with decreasing temperature (Petrich and Eiken, 2009). Hence, a temperature change may lead to convective mixing within the sea ice and underlying seawater, thereby coupling atmospheric exchange to conditions within

TCD
9, 45–75, 2015

the ice and ocean. Information on sea ice salinity, temperature, and therefore brine volume, were not available for the DNB site.

The observation of larger CO_2-fluxes at this site is consistent with the notion that the brine volume at the snow/ice interface was well above the threshold for vertical mixing, and therefore for CO_2 exchange with the atmosphere. The snow/ice interface was warmer during the DNB time series relative to the ICEI and POLYI stages of the experiment (Sects. 3.1–3.3), and therefore it is reasonable to assume that brine was present at the snow base and that processes affecting CO_2 speciation in the brine described above for POLYI remained active throughout the study period.

Recent findings by Santschi and Rossi (2006) suggest that CO_2 adsorption/desorption (exothermic/endothermic) onto $CaCO_3$ can occur at ambient temperature and is directly related to the amount of H_2O adsorption/desorption onto $CaCO_3$. This process can explain the strong correlation observed between latent heat fluxes and CO_2-fluxes at POLYI (Fig. 5g). Alternatively, the relationship could be coincidental given the simple fact the snow at POLYI was wet, providing a readily available water source for exchange to the atmosphere and therefore the latent heat flux could be unrelated to the carbon system of the site. To our knowledge no studies have described the properties of adsorption/desorption processes within snow, indicating that further work is needed to properly evaluate the influence, if any, of this process.

The correlation between R_{net} and CO_2-flux was more significant at POLYI (R^2 = 0.73, $p < 0.05$) relative to at DNB (R^2 = 0.40, $p < 0.05$). One explanation might be that the thinner snow-cover at POLYI (15–20 cm relative to 67–88 cm at DNB) allowed for greater transmission of incident solar radiation to the snow/ice interface. Another compelling explanation might be that wind played a much more central part in modifying exchanges at DNB, due to the much thicker snow-cover.

4.2.2 Wind-speed

Gas transport in snow occurs by way of diffusion, advection and thermal convection. While diffusion is a slow process, and thermal convection is a notoriously elusive pro-

TCD
9, 45–75, 2015

cess (Powers et al., 1985; Sturm, 1991), advection, or wind-pumping, is a dynamic process that allow for very rapid flushing of CO_2, which has been accumulated in the snow-pockets (Jones et al., 1999) following e.g. emission from the sea-ice. The wind pumping process has been described in a number of studies (Albert et al., 2002; Albert and Shultz, 2002; Jones et al., 1999; Massman and Frank, 2006; Seok et al., 2009; Takagi et al., 2005) as well as discussed specifically as a plausible mechanism for periods of enhanced CO_2 exchanges on sea-ice (Miller et al., 2011b; Papakyriakou and Miller, 2011). Given the indication of a strong relationship between CO_2-fluxes and site energy balance, an appropriate evaluation of wind pumping requires the separation of thermo-chemical influences from any wind pumping effects. In Fig. 6 the previously discussed correlations between CO_2-fluxes and net radiation (Fig. 5e, j, o) are re-evaluated in the context of wind-speed with marker color-coding corresponding to strength of wind-speed. At ICEI (Fig. 6a) no clear pattern exists between CO_2-fluxes and net radiation or wind-speed. This is consistent with the limited gas permeability of the upper sea-ice brines described previously for this site. At POLYI (Fig. 6b) a strong correlation between CO_2-fluxes and net radiation is evident, as described above, but no clear connection with wind-speed is evident. At DNB (Fig. 6c), however, two distinct mechanisms appear to be present. The two mechanisms are evident as a plausible relationship between net radiative forcing and CO_2-fluxes where $|F_{CO_2}| \leq 85\,\mathrm{mmol\,m^{-2}\,d^{-1}}$ coinciding with modest wind-speeds of $U \leq 8\,\mathrm{m\,s^{-1}}$, while the same relationship is negligible when $F_{CO_2} > 100\,\mathrm{mmol\,m^{-2}\,d^{-1}}$, coinciding with the strongest wind-speeds recorded $U = 10 \pm 2\,\mathrm{m\,s^{-1}}$. The implication is that wind-pumping is a plausible additional process at the DNB site. The absence of a similar pattern of wind-pumping at POLYI may be due to the fact that we were unable to observe frequent examples of CO_2 exchange in the presence of high winds, due to the limited timeframe of the experiment. Another interpretation might be that a thicker snow-cover, such as conditions at DNB, constitutes a greater potential for snow-cover pumping of stored CO_2. This view is consistent with the findings of Nomura et al. (2010) who suggest that the presence of snow serves as a lid on CO_2 exchanges. They reported fluxes measured by a chamber system and

TCD
9, 45–75, 2015

therefore would not have been able to resolve CO_2 transport and exchange via snow-pumping. It is our premise that snow would indeed inhibit CO_2 exchange if transport were limited to the slow process of molecular diffusion.

4.2.3 Diurnal flux patterns

Finally, we synthesize our findings by evaluating the diurnal evolution of radiative components, the sensible heat fluxes and the CO_2-fluxes. The results are similar at all sites, hence only the results from the DNB site are shown (Fig. 7). Here we get a much clearer impression of how the radiative components are related to CO_2-fluxes at different times of the day. Net shortwave radiation surplus drives surface and snow cover warming during the day (Fig. 7b), resulting in both sensible heat warming of the lower atmosphere (Fig. 7a) and long wave radiative emission (Fig. 7c). During night, long wave radiation deficit drives surface and snow cover cooling (Fig. 7c), resulting in sensible heat flux towards the surface (Fig. 7a). All three terms are seen to be strongly correlated with CO_2-fluxes; $R^2(F_{CO_2}, R_n^{SW}) = 0.42$, $R^2(F_{CO_2}, Q_{SENS}) = 0.86$ and $R^2(F_{CO_2}, R_n^{LW}) = 0.37$, all with $p < 0.05$. The diurnal pattern of net radiation is shown alongside the diurnal pattern of CO_2-fluxes in Fig. 7d. Here CO_2 outgassing is seen to coincide with net radiative cooling during most of the evening, night and morning (20:00–12:00) while some uptake coincides with net radiative warming during the remaining period (12:00–20:00). The plausible underlying thermochemical processes were discussed in Sect. 4.2.1. The correlation between CO_2-fluxes and net radiative forcing is seen to be less significant relative to the other components; $R^2(F_{CO_2}, R_{net}) = 0.23$ ($p < 0.05$). This is likely because of the additional amplification of CO_2-fluxes by snow-pumping processes during periods of strong winds (Sect. 4.2.2), seen in Fig. 7d to occur most frequently during the night. The fact that a clear diurnal pattern of CO_2-fluxes exists emphasizes that carbon budget estimates over sea ice should include measurements sufficiently frequent to resolve the flux and not be restricted to snapshot measurements during the day.

TCD
9, 45–75, 2015

5 Conclusion

Eddy covariance observations of CO_2-fluxes were conducted during late winter at three locations on fast ice and newly formed polynya ice in a coastal fjord environment in North East Greenland. For the first time, CO_2-flux estimates over sea ice were derived using the Ogive optimization method (Sievers et al., 2014) shown to be an appropriate technique for quantifying small fluxes. Observations at the three sites were indicative of an environment experiencing the slow onset and gradual intensification of spring warming with average net solar radiation increasing from $-27\,W\,m^{-2}$ at ICEI to $-40\,W\,m^{-2}$ at POLYI and $-75\,W\,m^{-2}$ at DNB. Concurrent CO_2-flux estimates increased throughout the period. ICEI was characterized by negligible net CO_2 fluxes $F_{CO_2} = 1.4 \pm 4.9\,mmol\,m^{-2}\,d^{-1}$ and limited flux variation, POLYI was characterized by net CO_2 uptake $F_{CO_2} = -3.4 \pm 31.4\,mmol\,m^{-2}\,d^{-1}$ and considerably stronger response to net radiative forcing and wind-speed, and DNB was characterized by net CO_2 outgassing $F_{CO_2} = 36.7 \pm 72.8\,mmol\,m^{-2}\,d^{-1}$ and a strong response to net radiative forcing and wind-speed. A correlation analysis supports a connection between site energetics, wind-speed and CO_2-fluxes linked to a number of possible thermally driven processes, including brine volume expansion/contraction, brine dissolution/concentration and calcium carbonate formation/dissolution as well as wind-venting of the snow-cover. In addition, a strong relationship between latent heat and CO_2-fluxes was found at POLYI, suggesting the presence of CO_2 adsorption/desorption processes in moist snow. Finally a strong diurnal relationship between site energetics and CO_2-fluxes was found, highlighting the importance of conducting observations throughout the day in order to estimate properly the carbon exchange budget over sea-ice.

Acknowledgements. The study received financial support from the Arctic Research Centre, Aarhus University, the DEFROST project of the Nordic Centre of Excellence program "Interaction between Climate Change and the Cryosphere", the collaborative research project "Changing Permafrost in the Arctic and its Global Effects in the 21st century" (PAGE21), the Canada Excellence Research Chair program, the Natural Sciences and Engineering Research Council

TCD
9, 45–75, 2015

of Canada (NSERC) and the ArcticNet Canadian network of centres of excellence. Additionally, this work is a contribution to the Arctic Science Partnership (ASP). We wish to thank the Greenland Survey (ASIAQ) for the use of radiation observations from the Zackenberg Research station. D. H. Søgaard was supported financially by the Commission for Scientific Research in Greenland (KVUG). The authors furthermore wish to thank a number of people who assisted with the Daneborg experiment; Bruce Johnson, Kunuk Lennert, Ivali Lennert, Egon Randa Frandsen, Jens Ehn and Karl Attard.

References

Albert, M. R. and Shultz, E. F.: Snow and firn properties and air-snow transport processes at Summit, Greenland, Atmos. Environ., 36, 2789–2797, doi:10.1016/S1352-2310(02)00119-X, 2002.

Albert, M. R., Grannas, A. M., Bottenheim, J., Shepson, P. B., and Perron, F. E.: Processes and properties of snow-air transfer in the high Arctic with application to interstitial ozone at Alert, Canada, Atmos. Environ., 36, 2779–2787, doi:10.1016/S1352-2310(02)00118-8, 2002.

Anderson, L. G., Falck, E., Jones, E. P., Jutterström, S., and Swift, J. H.: Enhanced uptake of atmospheric CO_2 during freezing of seawater: a field study in Storfjorden, Svalbard, J. Geophys. Res.-Oceans, 109, C06004, doi:10.1029/2003JC002120, 2004.

Baldocchi, D.: Breathing of the terrestrial biosphere: lessons learned from a global network of carbon dioxide flux measurement systems, Aust. J. Bot., 56, 1–26, doi:10.1071/Bt07151, 2008.

Barber, D. G., Papakyriakou, T. N., Ledrew, E. F., and Shokr, M. E.: An examination of the relation between the spring period evolution of the scattering coefficient (sigma-degrees) and radiative fluxes over landfast sea-ice, Int. J. Remote Sens., 16, 3343–3363, 1995a.

Barber, D. G., Reddan, S. P., and Ledrew, E. F.: Statistical characterization of the geophysical and electrical-properties of snow on landfast first-year sea-ice, J. Geophys. Res.-Oceans, 100, 2673–2686, doi:10.1029/94jc02200, 1995b.

Barber, D. G., Ehn, J. K., Pućko, M., Rysgaard, S., Deming, J. W., Bowman, J. S., Papakyriakou, T., Galley, R. J., and Søgaard, D. H.: Frost flowers on young Arctic sea ice: the climatic, chemical and microbial significance of an emerging ice type, J. Geophys. Res.-Atmos., 119, 11593–11612, doi:10.1002/2014JD021736, 2014.

TCD
9, 45–75, 2015

Crocker, G. B.: A physical model for predicting the thermal-conductivity of brine-wetted snow, Cold Reg. Sci. Technol., 10, 69–74, doi:10.1016/0165-232x(84)90034-X, 1984.
Delille, B., Jourdain, B., Borges, A. V., Tison, J. L., and Delille, D.: Biogas (CO_2, O_2^-, dimethylsulfide) dynamics in spring Antarctic fast ice, Limnol. Oceanogr., 52, 1367–1379, doi:10.4319/lo.2007.52.4.1367, 2007.
Desjardins, R. L., Macpherson, J. I., Schuepp, P. H., and Karanja, F.: An evaluation of aircraft flux measurements of Co_2, water-vapor and sensible heat, Bound.-Lay. Meteorol., 47, 55–69, doi:10.1007/Bf00122322, 1989.
Dieckmann, G. S., Nehrke, G., Papadimitriou, S., Gottlicher, J., Steininger, R., Kennedy, H., Wolf-Gladrow, D., and Thomas, D. N.: Calcium carbonate as ikaite crystals in Antarctic sea ice, Geophys. Res. Lett., 35, L08501, doi:10.1029/2008gl033540, 2008.
Else, B. G. T., Papakyriakou, T. N., Galley, R. J., Drennan, W. M., Miller, L. A., and Thomas, H.: Wintertime CO_2 fluxes in an Arctic polynya using eddy covariance: evidence for enhanced air–sea gas transfer during ice formation, J. Geophys. Res.-Oceans, 116, C00g03, doi:10.1029/2010jc006760, 2011.
Else, B. G. T., Papakyriakou, T. N., Raddatz, R., Galley, R. J., Mundy, C. J., Barber, D. G., Swystun, K., and Rysgaard, S.: Surface energy budget of landfast sea ice during the transitions from winter to snowmelt and melt pond onset: the importance of net longwave radiation and cyclone forcings, J. Geophys. Res.-Oceans, 119, 3679–3693, doi:10.1002/2013JC009672, 2014.
Fischer, M., Thomas, D. N., Krell, A., Nehrke, G., Gottlicher, J., Norman, L., Meiners, K. M., Riaux-Gobin, C., and Dieckmann, G. S.: Quantification of ikaite in Antarctic sea ice, Antarct Sci., 25, 421–432, doi:10.1017/S0954102012001150, 2013.
Foken, T., Wimmer, F., Mauder, M., Thomas, C., and Liebethal, C.: Some aspects of the energy balance closure problem, Atmos. Chem. Phys., 6, 4395–4402, doi:10.5194/acp-6-4395-2006, 2006.
Ganot, Y., Dragila, M. I., and Weisbrod, N.: Impact of thermal convection on CO_2 flux across the Earth–atmosphere boundary in high-permeability soils, Agr. Forest Meteorol., 184, 12–24, doi:10.1016/j.agrformet.2013.09.001, 2014.
Geilfus, N. X., Carnat, G., Papakyriakou, T., Tison, J. L., Else, B., Thomas, H., Shadwick, E., and Delille, B.: Dynamics of pCO_2 and related air–ice CO_2 fluxes in the Arctic coastal zone (Amundsen Gulf, Beaufort Sea), J. Geophys. Res.-Oceans, 117, C00g10, doi:10.1029/2011jc007118, 2012.

TCD
9, 45–75, 2015

Geilfus, N. X., Carnat, G., Dieckmann, G. S., Halden, N., Nehrke, G., Papakyriakou, T., Tison, J. L., and Delille, B.: First estimates of the contribution of $CaCO_3$ precipitation to the release of CO_2 to the atmosphere during young sea ice growth, J. Geophys. Res.-Oceans, 118, 244–255, doi:10.1029/2012JC007980, 2013.

Golden, K. M., Ackley, S. F., and Lytle, V. I.: The percolation phase transition in sea ice, Science, 282, 2238–2241, doi:10.1126/science.282.5397.2238, 1998.

Jones, H. G., Pomeroy, J. W., Davies, T. D., Tranter, M., and Marsh, P.: CO_2 in Arctic snow cover: landscape form, in-pack gas concentration gradients, and the implications for the estimation of gaseous fluxes, Hydrol. Process., 13, 2977–2989, 1999.

Killawee, J. A., Fairchild, I. J., Tison, J. L., Janssens, L., and Lorrain, R.: Segregation of solutes and gases in experimental freezing of dilute solutions: implications for natural glacial systems, Geochim. Cosmochim. Ac., 62, 3637–3655, doi:10.1016/S0016-7037(98)00268-3, 1998.

Lizotte, M. P.: The contributions of sea ice algae to Antarctic marine primary production, Am. Zool., 41, 57–73, doi:10.1668/0003-1569(2001)041[0057:Tcosia]2.0.Co;2, 2001.

Loose, B., Miller, L. A., Elliott, S., and Papakyriakou, T.: Sea ice biogeochemistry and material transport across the frozen interface, Oceanography, 24, 202–218, 2011a.

Loose, B., Schlosser, P., Perovich, D., Ringelberg, D., Ho, D. T., Takahashi, T., Richter-Menge, J., Reynolds, C. M., McGillis, W. R., and Tison, J. L.: Gas diffusion through columnar laboratory sea ice: implications for mixed-layer ventilation of CO_2 in the seasonal ice zone, Tellus B, 63, 23–39, doi:10.1111/j.1600-0889.2010.00506.x, 2011b.

Marion, G. M.: Carbonate mineral solubility at low temperatures in the Na-K-Mg-Ca-H-Cl-SO_4-OH-HCO_3-CO_3-CO_2-H_2O system, Geochim. Cosmochim. Ac., 65, 1883–1896, doi:10.1016/S0016-7037(00)00588-3, 2001.

Massman, W. J. and Frank, J. M.: Advective transport of CO_2 in permeable media induced by atmospheric pressure fluctuations: 2. Observational evidence under snowpacks, J. Geophys. Res.-Biogeo., 111, G03005, doi:10.1029/2006jg000164, 2006.

Miller, L. A., Carnat, G., Else, B. G. T., Sutherland, N., and Papakyriakou, T. N.: Carbonate system evolution at the Arctic Ocean surface during autumn freeze-up, J. Geophys. Res.-Oceans, 116, C00g04, doi:10.1029/2011jc007143, 2011a.

Miller, L. A., Papakyriakou, T. N., Collins, R. E., Deming, J. W., Ehn, J. K., Macdonald, R. W., Mucci, A., Owens, O., Raudsepp, M., and Sutherland, N.: Carbon dynamics in sea ice: a win-

TCD
9, 45–75, 2015

ter flux time series, J. Geophys. Res.-Oceans, 116, C02028, doi:10.1029/2009jc006058, 2011b.
Nomura, D., Yoshikawa-Inoue, H., and Toyota, T.: The effect of sea-ice growth on air–sea CO_2 flux in a tank experiment, Tellus B, 58, 418–426, doi:10.1111/j.1600-0889.2006.00204.x, 2006.
Nomura, D., Assmy, P., Nehrke, G., Granskog, M. A., Fischer, M., Dieckmann, G. S., Fransson, A., Hu, Y. B., and Schnetger, B.: Characterization of ikaite ($CaCO_3 \cdot 6H_2O$) crystals in first-year Arctic sea ice north of Svalbard, Ann. Glaciol., 54, 125–131, doi:10.3189/2013aog62a034, 2013.
Papadimitriou, S., Kennedy, H., Kattner, G., Dieckmann, G. S., and Thomas, D. N.: Experimental evidence for carbonate precipitation and CO_2 degassing during sea ice formation, Geochim. Cosmochim. Ac., 68, 1749–1761, doi:10.1016/j.gca.2003.07.004, 2004.
Papakyriakou, T. and Miller, L.: Springtime CO_2 exchange over seasonal sea ice in the Canadian Arctic Archipelago, Ann. Glaciol., 52, 215–224, 2011.
Parmentier, F. J. W., Christensen, T. R., Sorensen, L. L., Rysgaard, S., McGuire, A. D., Miller, P. A., and Walker, D. A.: The impact of lower sea-ice extent on Arctic greenhouse-gas exchange, Nat. Clim. Change, 3, 195–202, doi:10.1038/Nclimate1784, 2013.
Perovich, D. K. and Richtermenge, J. A.: Surface characteristics of lead ice, J. Geophys. Res.-Oceans, 99, 16341–16350, doi:10.1029/94jc01194, 1994.
Persson, P. O. G.: Onset and end of the summer melt season over sea ice: thermal structure and surface energy perspective from SHEBA, Clim. Dynam., 39, 1349–1371, doi:10.1007/s00382-011-1196-9, 2012.
Petrich, C. and Eiken, H.: Growth, structure and properties of sea ice, in: Sea Ice, edited by: Thomas, D. N. and Dieckmann, G. S., Wiley-Blackwell, Oxford, UK, 23–77, 2009.
Powers, D., Colbeck, S. C., and Oneill, K.: Experiments on thermal-convection in snow, Ann. Glaciol., 6, 43–47, 1985.
Rysgaard, S., Glud, R. N., Sejr, M. K., Bendtsen, J., and Christensen, P. B.: Inorganic carbon transport during sea ice growth and decay: a carbon pump in polar seas, J. Geophys. Res.-Oceans, 112, C03016, doi:10.1029/2006jc003572, 2007.
Rysgaard, S., Bendtsen, J., Pedersen, L. T., Ramlov, H., and Glud, R. N.: Increased CO_2 uptake due to sea ice growth and decay in the Nordic Seas, J. Geophys. Res.-Oceans, 114, C09011, doi:10.1029/2008jc005088, 2009.

TCD
9, 45–75, 2015

Rysgaard, S., Bendtsen, J., Delille, B., Dieckmann, G. S., Glud, R. N., Kennedy, H., Mortensen, J., Papadimitriou, S., Thomas, D. N., and Tison, J. L.: Sea ice contribution to the air–sea CO_2 exchange in the Arctic and Southern Oceans, Tellus B, 63, 823–830, doi:10.1111/j.1600-0889.2011.00571.x, 2011.

Rysgaard, S., Glud, R. N., Lennert, K., Cooper, M., Halden, N., Leakey, R. J. G., Hawthorne, F. C., and Barber, D.: Ikaite crystals in melting sea ice – implications for pCO_2 and pH levels in Arctic surface waters, The Cryosphere, 6, 901–908, doi:10.5194/tc-6-901-2012, 2012.

Rysgaard, S., Søgaard, D. H., Cooper, M., Pućko, M., Lennert, K., Papakyriakou, T. N., Wang, F., Geilfus, N. X., Glud, R. N., Ehn, J., McGinnis, D. F., Attard, K., Sievers, J., Deming, J. W., and Barber, D.: Ikaite crystal distribution in winter sea ice and implications for CO_2 system dynamics, The Cryosphere, 7, 707–718, doi:10.5194/tc-7-707-2013, 2013.

Santschi, C. and Rossi, M. J.: Uptake of CO_2, SO_2, HNO_3 and HCl on calcite ($CaCO_3$) at 300 K: mechanism and the role of adsorbed water, J. Phys. Chem. A, 110, 6789–6802, doi:10.1021/Jp056312b, 2006.

Semiletov, I., Makshtas, A., Akasofu, S. I., and Andreas, E. L.: Atmospheric CO_2 balance: the role of Arctic sea ice, Geophys. Res. Lett., 31, L05121, doi:10.1029/2003gl017996, 2004.

Semiletov, I. P., Pipko, I. I., Repina, I., and Shakhova, N. E.: Carbonate chemistry dynamics and carbon dioxide fluxes across the atmosphere–ice–water interfaces in the Arctic Ocean: pacific sector of the Arctic, J. Marine Syst., 66, 204–226, doi:10.1016/j.jmarsys.2006.05.012, 2007.

Seok, B., Helmig, D., Williams, M. W., Liptzin, D., Chowanski, K., and Hueber, J.: An automated system for continuous measurements of trace gas fluxes through snow: an evaluation of the gas diffusion method at a subalpine forest site, Niwot Ridge, Colorado, Biogeochemistry, 95, 95–113, doi:10.1007/s10533-009-9302-3, 2009.

Sievers, J., Papakyriakou, T., Larsen, S., Jammet, M. M., Rysgaard, S., Sejr, M. K., and Sørensen, L. L.: Estimating local atmosphere-surface fluxes using eddy covariance and numerical Ogive optimization, Atmos. Chem. Phys. Discuss., 14, 21387–21432, doi:10.5194/acpd-14-21387-2014, 2014.

Sogaard, D. H., Thomas, D. N., Rysgaard, S., Glud, R. N., Norman, L., Kaartokallio, H., Juul-Pedersen, T., and Geilfus, N. X.: The relative contributions of biological and abiotic processes to carbon dynamics in subarctic sea ice, Polar Biol., 36, 1761–1777, doi:10.1007/s00300-013-1396-3, 2013.

TCD
9, 45–75, 2015

Sturm, M.: The role of thermal convection in heat and mass transport in the subarctic snow-cover, Cold Regions Research and Engineering Laboratory (US), Army Corps of Engineers Cold Regions Research & Engineering Laboratory, CRREL Technical Report 91-19, 1991.

Sturm, M., Perovich, D. K., and Holmgren, J.: Thermal conductivity and heat transfer through the snow on the ice of the Beaufort Sea, J. Geophys. Res.-Oceans, 107, 8043, doi:10.1029/2000jc000409, 2002.

Sørensen, L. L., Jensen, B., Glud, R. N., McGinnis, D. F., Sejr, M. K., Sievers, J., Søgaard, D. H., Tison, J.-L., and Rysgaard, S.: Parameterization of atmosphere–surface exchange of CO_2 over sea ice, The Cryosphere, 8, 853–866, doi:10.5194/tc-8-853-2014, 2014.

Takagi, K., Nomura, M., Ashiya, D., Takahashi, H., Sasa, K., Fujinuma, Y., Shibata, H., Akibayashi, Y., and Koike, T.: Dynamic carbon dioxide exchange through snowpack by wind-driven mass transfer in a conifer-broadleaf mixed forest in northernmost Japan, Global Biogeochem. Cy., 19, Gb2012, doi:10.1029/2004gb002272, 2005.

Thomas, D. N. and Dieckmann, G. S.: Sea Ice, 2 edn., Wiley-Blackwell, Oxford, 2010.

Tison, J. L., Haas, C., Gowing, M. M., Sleewaegen, S., and Bernard, A.: Tank study of physico-chemical controls on gas content and composition during growth of young sea ice, J. Glaciol., 48, 177–191, doi:10.3189/172756502781831377, 2002.

Vancoppenolle, M., Goosse, H., de Montety, A., Fichefet, T., Tremblay, B., and Tison, J. L.: Modeling brine and nutrient dynamics in Antarctic sea ice: the case of dissolved silica, J. Geophys. Res.-Oceans, 115, C02005, doi:10.1029/2009jc005369, 2010.

Zemmelink, H. J., Delille, B., Tison, J. L., Hintsa, E. J., Houghton, L., and Dacey, J. W. H.: CO_2 deposition over the multi-year ice of the western Weddell Sea, Geophys. Res. Lett., 33, L13606, doi:10.1029/2006gl026320, 2006.

Zhou, J., Delille, B., Eicken, H., Vancoppenolle, M., Brabant, F., Carnat, G., Geilfus, N.-X., Papakyriakou, T., Heinesch, B., and Tison, J.-L.: Physical and biogeochemical properties in landfast sea ice (Barrow, Alaska): insights on brine and gas dynamics across seasons, J. Geophys. Res.-Oceans, 118, 3172–3189, doi:10.1002/jgrc.20232, 2013.

TCD
9, 45–75, 2015

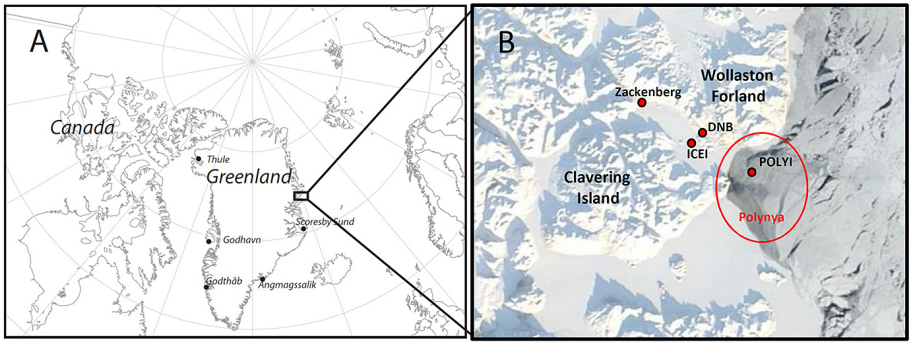

Figure 1. (a) Regional and **(b)** local overview of field-sites in Young-Sound, NE Greenland. Sites ICEI and DNB were located in the inner-fjord characterized by thick fast sea ice and a thick snow-cover, and POLYI was located in an active polynia, characterized by thin ice and snow-cover.

TCD
9, 45–75, 2015

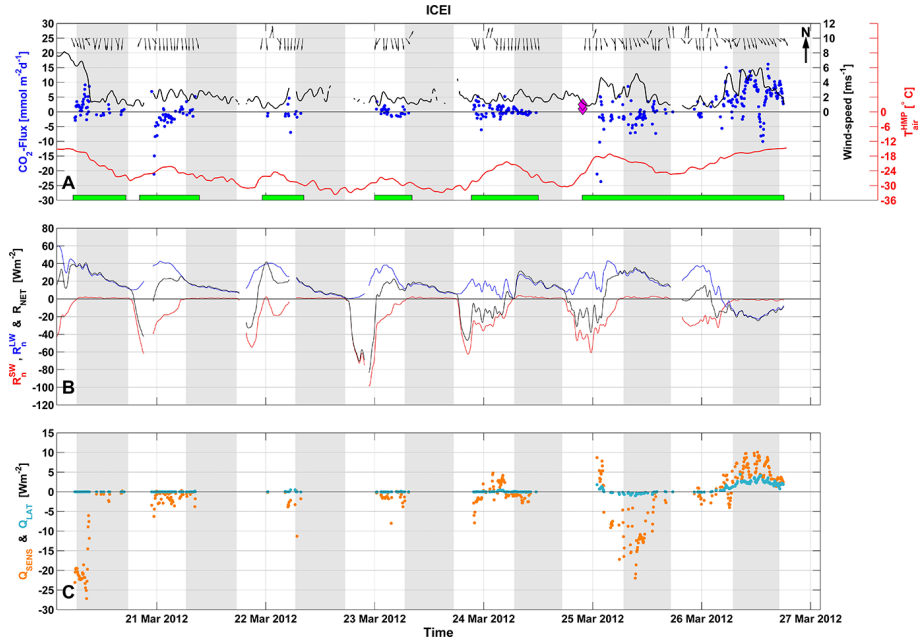

Figure 2. ICEI timeseries of **(a)** EC derived CO_2-fluxes (blue markers), chamber observations of CO_2-flux (magenta diamonds), wind-speed (black line), HMP air temperature (red line) and wind-direction (black arrows). Wind-direction due north is indicated in the upper right corner. Green bars indicate when the EC instruments were online; **(b)** net shortwave radiation (red line), net longwave radiation (blue line) and net radiation (black line); **(c)** turbulent sensible heat flux (orange dots) and turbulent latent heat flux (light-blue dots). Grey shaded areas indicate night-time.

TCD
9, 45–75, 2015

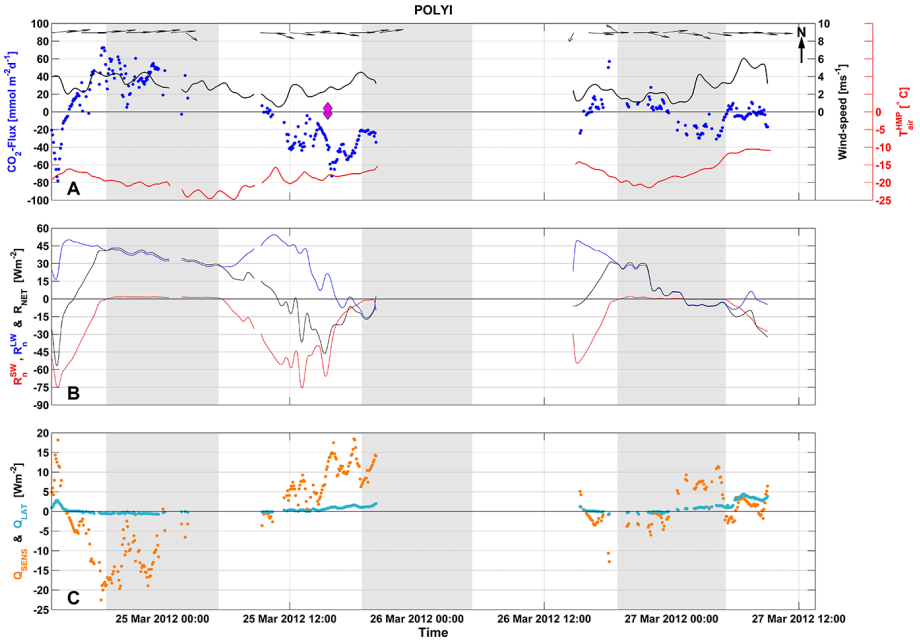

Figure 3. POLYI timeseries of **(a)** EC derived CO_2-fluxes (blue markers), chamber observations of CO_2-flux (magenta diamonds), HMP air temperature (red line), wind-speed (black line) and wind-direction (black arrows); wind-direction due north is indicated in the upper right corner. **(b)** Net shortwave radiation (red line), net longwave radiation (blue line) and net radiation (black line); **(c)** turbulent sensible heat flux (orange dots) and turbulent latent heat flux (light-blue dots). Grey shaded areas indicate night-time.

TCD
9, 45–75, 2015

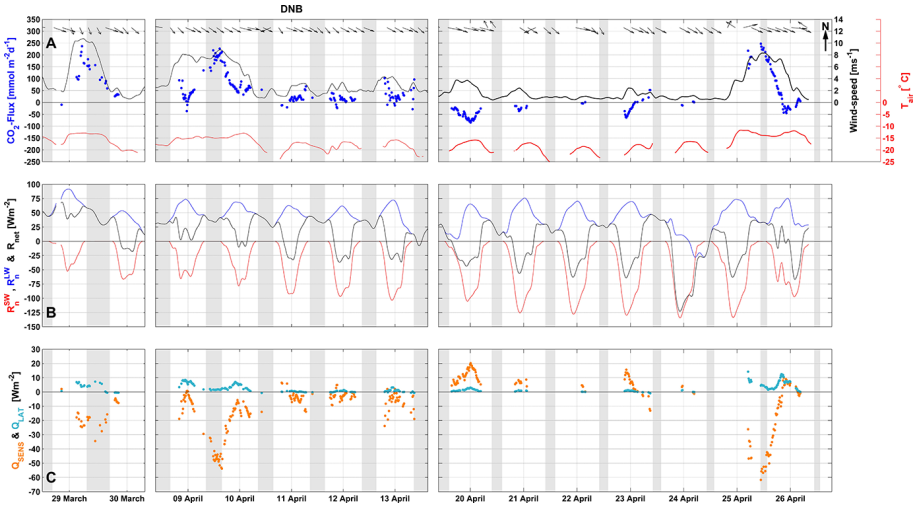

Figure 4. DNB timeseries of **(a)** EC derived CO_2-fluxes (blue markers), sonic air temperature (red line), wind-speed (black line) and wind-direction (black arrows); wind-direction due north is indicated in the upper right corner. **(b)** Net shortwave radiation (red line), net longwave radiation (blue line) and net radiation (black line); **(c)** turbulent sensible heat flux (orange dots) and turbulent latent heat flux (light-blue dots). Grey shaded areas indicate night-time.

TCD
9, 45–75, 2015

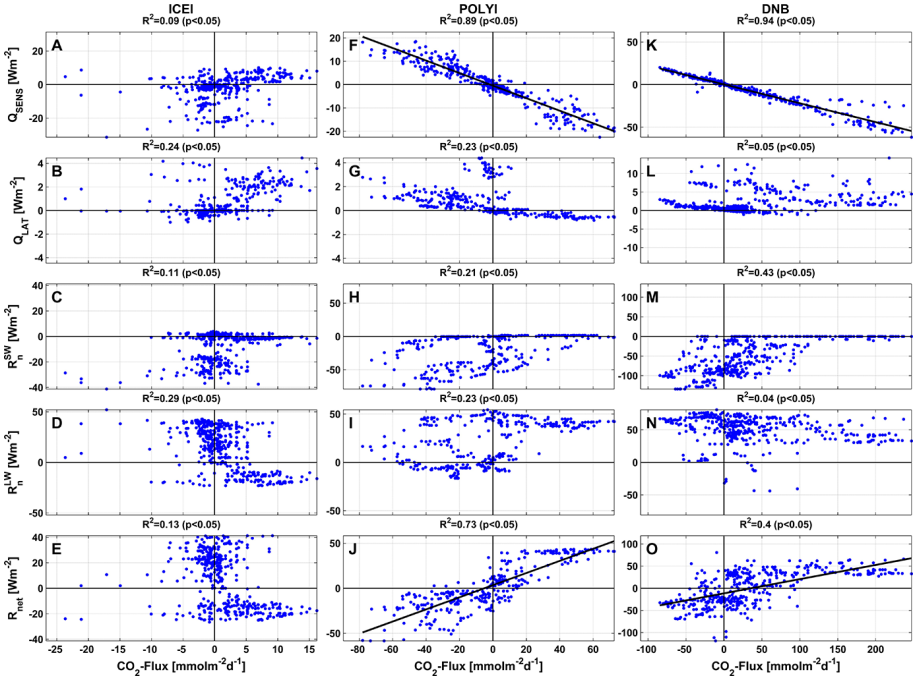

Figure 5. Correlations between components of the energy balance (rows) and CO_2-fluxes at all three sites (columns). Correlations for all observations are listed in black.

TCD
9, 45–75, 2015

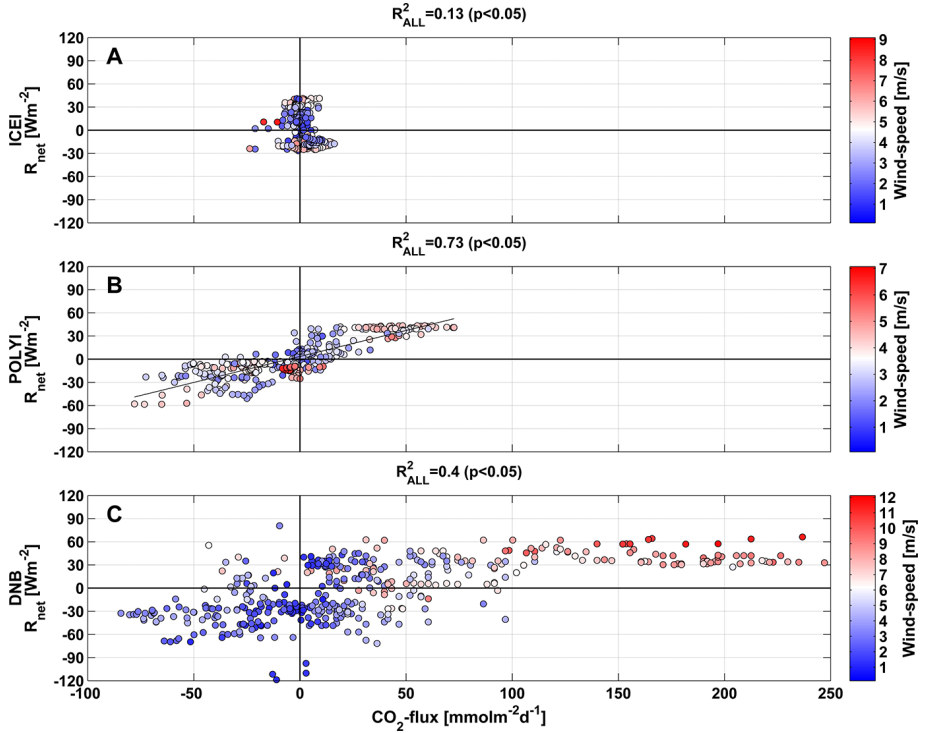

Figure 6. Correlations between net radiative forcing and CO_2-flux at sites **(a)** ICEI; **(b)** POLYI and **(c)** DNB, with color-coded markers indicating wind-speed according to the respective colorbars.

TCD
9, 45–75, 2015

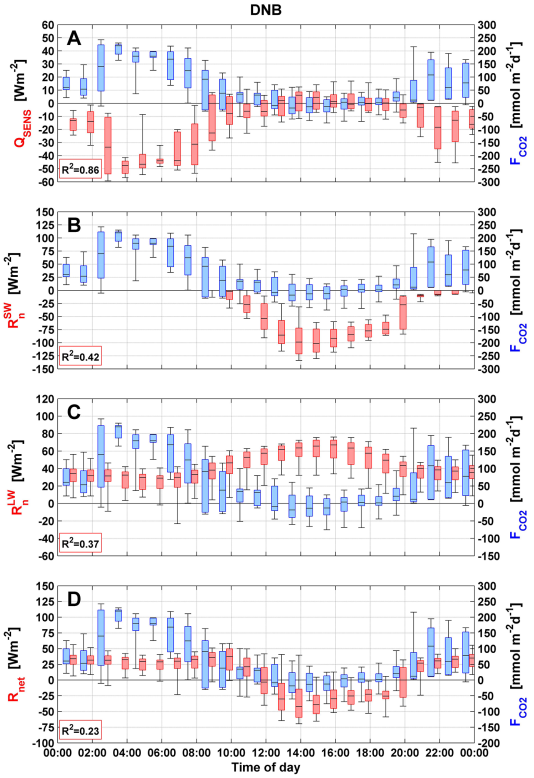

Figure 7. Diurnal patterns of **(a)** sensible heat flux **(b)** net shortwave energy **(c)** net longwave energy and **(d)** net radiative energy (red boxplots) shown alongside the diurnal pattern of CO_2-fluxes (blue boxplots) for the DNB site. Boxplots are composed of the median (black middle line), the 25–75th percentile (box) and the 9–91st percentile (black whiskers) respectively. Correlations are indicated in red boxes in the lower-left corner of each graph.

TCD
9, 45–75, 2015